

REPORT CCG 71-57, NBS 2210471

NBSIR 74-531-566

ULTRASONIC INTERFEROMETER MANOMETER

P. Heydemann

Pressure and Vacuum Section
Heat Division, NBS
Washington, D.C. 20234

July 1974

Annual report for period July 1, 1973 - June 30, 1974

Prepared for CCG - Army/Navy

OBJECTIVE

It is the objective of this project to develop, design and construct a mercury manometer covering the range from 2 to 2300 mmHg with an accuracy of $\pm 10 \mu\text{m}$ for 2 to 1000 mmHg, $\pm 20 \mu\text{m}$ for 1000 to 1500 mmHg, $\pm 30 \mu\text{m}$ for 1500 to 2300 mmHg. The ultrasonic fringe counting interferometer shall be adapted to this application.

Such a manometer would be useful as a standard manometer in calibration laboratories. It would be capable of automatic operation. Its analog or digital output could be used as input to a very stable pressure controller in an automatic calibration stand. Even over long periods of use only the thermometers and a crystal oscillator need to be recalibrated, a task that can readily be performed in most laboratories.

The principle of the ultrasonic fringe counting interferometer is as follows: A short wavetrain ($50 \mu\text{s}$) with a very well known carrier frequency (10 MHz) is launched from a transducer at the bottom of the mercury column into the mercury. The pulse is reflected at the surface and received and converted into an electrical signal again by the transducer. Part of the pulse energy is reflected into the column again and again. Each time an echo impinges upon the transducer an analog electrical signal is generated. The received signals are phase sensitive detected in two detectors with a 90° phase shift between the reference signals. The resulting output signal is a vector. Its amplitude depends on the amplitude of the received echo. Its phase depends on the length L of the mercury column. A change of column length equal to $\lambda/2$, where λ is the sound wavelength, causes the output vector to rotate by 2π . An electronic counter circuit can be designed that recognizes the direction of rotation and generates one count for each $\pi/4$ rotation. If echos other than the first are used, one count per $\pi/4p$ rotation is generated, where p is the order of the echo.

With a carrier frequency of 9 MHz and a speed of sound in mercury of about 1500 m/s the following resolution per count is expected:

1st echo : 20 μm
2nd echo : 10 μm
4th echo : 5 μm
10th echo : 2 μm .

Instead of using echos of very high order number it may be more expedient to interpolate between counts with a direct phase measurement.

The accuracy of the measurement depends to a large extent upon the accuracy with which the speed of sound in mercury is known. The best presently available data indicate a precision of about 1 part in 10,000, but no estimate of systematic uncertainty is available and it is therefore imperative to perform speed of sound measurements of the highest possible accuracy.

The laser interferometer manometer now under construction at NBS will be used to perform such measurements and an accuracy approaching a few parts per million is expected.

ABSTRACT

The developments during this report period led to the design of a W-tube manometer with a maximum column length of 115cm. Two different ways of measuring the acoustical length of the columns were tested and precise measurements of the speed of sound in mercury were made.

INTRODUCTION

In this report we shall describe the W-tube manometer and the measurements made with it without going into great detail about individual problems encountered and solved. These have been dealt with in two quarterly reports.

The effort described in this report was supported in part by funds from the CCG. Substantial funding was obtained through regular STRS allocation from NBS.

DESIGN OF THE W-TUBE MANOMETER

Fig. 1 shows a schematic of the W-tube manometer. The manometer is mounted on a truncated-triangular stainless steel baseplate with three adjustable supports. Large holes are provided for the bottom closure flanges. A rectangular mounting plate, ground plane and parallel, serves as reference plane for the bottom closure. It also carries the three manometer tubes. The three manometer tubes are connected through lateral holes with welded-in tubulations, appropriate fittings and tubes all made of stainless steel.

The three manometer tubes are sealed against the mounting plate and the top closures with polytetrafluoroethylene washers. Each tube is tightened down with four screw rods anchored in the mounting plate. The glass tubes have an outer diameter of ⁶²~~52~~ mm and an inner diameter of 50 mm. Their length is 600 mm for the outer columns and 1150 mm for the long center column.

Fig. 2 shows a cut through a bottom closure. The closure plates are 65 mm in diameter, 6mm thick and consist of titanium. The titanium disks are sealed against the mounting plate with O-rings. Flange rings are used to press the titanium disks flush against the mounting plate to ensure that all three closure disks are parallel to each other. The single-crystal quartz transducers are bonded to the closure plates with epoxy bonds.

Immediately before assembly all parts must be carefully cleaned and degreased. Particular attention must be paid to the closure plates. After degreasing they are etched with a solution of 25 to 30% HNO_3 and 2% HF in water followed by thorough rinsing with distilled water. Carefully and recently cleaned mercury must be used. The acoustic coupling between the closure plates and the mercury will improve for several days after filling the manometer with mercury.

The manometer is placed on a 60 mm thick plywood plate resting on top of a stone foundation. For additional isolation from structure-borne sound square foam-rubber pads 12 mm thick and 35 mm on edge were placed under the dishes carrying the adjustable supports. This provides sufficient vibration isolation to work even with the longest columns.

Horizontal adjustment of the mounting plate is achieved with a sensitive spirit level placed on the plate and appropriate adjustment of the support screws. Final adjustment is made by watching the undetected echo sequence on an oscilloscope and adjusting for uniform and small decay of the echos. Fig. 3 gives examples for a well adjusted plate and for one tilted about 0.04 degrees.

PNEUMATIC CONNECTIONS

To conveniently operate the manometer for experimental purposes the manometer was connected as shown in Fig. 4. The system of valves allows one to pressurize or release either side of the manometer relative to the other keeping it under helium pressure at all times. Thus the contamination of the mercury is kept to a minimum and smooth travel of the menisci is maintained.

A motor-driven valve in the mercury line to the center column can be used to arrest the manometer at any column length without disturbing the surfaces. This is particularly useful for the more time-consuming excess fringe measurements.

The burst pressure of the glass tubes is 180 psi or more as determined from

experiments with five annealed and unannealed tubes.

ACOUSTIC PERFORMANCE

Of great concern in the development of a long column manometer is the attenuation of the acoustic signal through the length of the mercury column. Measurements of the apparent attenuation, including the effects of beam spread and diffraction were made and the results are shown in Fig. 5. Here we have plotted the amplitude of the first echo as a function of column length in arbitrary units. Also plotted is the decrement, that is the amplitude ratio of successive echos, versus the length of the column. As the column length changes from 100 to 1100 mm the amplitude decreases from 1 to about .3 and the decrement rises from 1.6 to 5.7. At column lengths above about 300 mm it is not practical to work with echos other than the first.

Fig. 6.a to 6.1 shows CRT photographs of the echo sequences at various column lengths. Note that the sweep rates have been adjusted to show three echos. The vertical sensitivity settings have been left undisturbed. The variation of the echo amplitudes is small enough to be compressed to a near constant amplitude by a hard-limiting, tuned amplifier.

The tubes used in this manometer have not been coated with chromium or other conductive layers on the inside as an anti-static measure. Nevertheless the surfaces are quiet enough even when moving to maintain a running fringe count. The maximum rate of change of pressure applied was 4.5 mm Hg/s. For practical purposes ^{1 mm Hg/s} ~~half this~~ ~~rate~~ should not be exceeded.

It was found that the long column is easily excited to oscillations by structure-borne sound causing large enough ripples on the surface to make the interferometer fail. Placing the manometer on foam rubber pads improved the situation ^{sufficiently} ~~markedly~~.

ACOUSTIC LENGTH MEASUREMENT

The ultrasonic interferometric length measurement is based on the following principles: a short (50 μ s) acoustical wavetrain with constant carrier frequency (10 MHz) is radiated into the column, reflected at the surface, received, converted into an electrical signal and amplified. The phase of the received echo is compared with the carrier. This phase changes by 2π whenever the column length changes by half the wavelength of the acoustic wave. By deriving analog signals for the phase a count of half wavelength can be obtained. Two analog signals in quadrature can be used to discriminate between upwards and downwards movements.

It is obvious from the foregoing that the count begins with zero at some arbitrary length, which could, for example, be the equilibrium position of all columns with no differential pressure applied. If for any reason the acoustic signal is interrupted during the operation of the manometer, the continuous count is not maintained, the columns must be returned to equilibrium and the counter must be reset to zero. If this happens frequently and even at reasonably low rates of change of pressure, it will make the use of this manometer quite impractical. While we found that in the present set-up loss of continuous count is not a problem we nevertheless investigated ways of acoustically determining the length without reliance on an accumulated count.

There are two other methods which at least in principle can be applied here. The first is an interferometer method making use of the fact that the wavelength of the acoustic wave can be adjusted so that

$$n\lambda_n = 2L, \lambda_n = c/f_n$$

where n is an integer, λ is the wavelength, L is the length of the column, c is the speed of sound in mercury and f_n is a frequency. The f_n can be recognized in a system employing phase sensitive detection by the fact that all detected echos go through zero at this frequency provided that phase shifts in the electronic apparatus are properly compensated.

To solve the above equation for L we must determine n , which is always an integer, obtain c with sufficient accuracy from other measurements, and measure f_n for at least one n .

The f_n can be set to about 4 Hz. The f_n are about 10 MHz. The speed of sound c is known to about .01%. This must be improved by about two orders of magnitude. n , which for a one meter column is about 15,000, must be determined and herein lies the difficulty.

We have

$$f_n = \frac{nc}{2L}, \quad \frac{c}{2L} = f_1$$

$$f_n = nf_1.$$

If measurements are made at f_n and f_{n+m} we have

$$f_n = nf_1, \quad f_{n+m} = (n+m)f_1$$

and

$$f_{n+m} - f_n = mf_1.$$

This permits one to calculate f_1 provided m is known. m can be counted by going from one critical frequency adjustment to either the next, or the tenth, or the hundredth. With f_1 known we can calculate n from

$$n = \frac{f_n}{f_1}.$$

Written in closed form we have then

$$L = \frac{cm}{2(f_{n+m} - f_n)} \quad \text{or} \quad L = \frac{cn}{2f_n}$$

There are several ways to determine m accurately and several of these are presently being explored. In any case m is an integer and no uncertainty will be assigned to it. The frequency difference in the denominator of the left equation is limited by the usable bandwidth of the apparatus to about 150 kHz. Since the frequencies f_{n+m} and f_n can be determined to about 4 Hz, the uncertainty of the difference will be about 8 Hz/150 kHz or 50 ppm. This is clearly too large.

The second equation has an uncertainty - neglecting that due to the speed of sound and of n - of only 4 Hz/10 MHz or .4 ppm, but it requires the determination of n . How this can be done is illustrated in Appendix A with data taken recently with the long column.

A second interferometer method operates on the fractional fringes method.

Here one operates with several fixed and well-known wavelengths sent out sequentially into the column of unknown length L . When the reflected signals are picked up at the receiver their phase shifts relative to the transmitted signal will be $\theta = n \times 2\pi + g_n$. The column length can be calculated from

$$L = \frac{\theta}{2\pi} \times \frac{\lambda_n}{2} = \left(n + \frac{g_n}{2\pi}\right) \frac{\lambda_n}{2}$$

One assumes now that a small number of wavelengths can be found, which produce a unique set of fringe fractions g_n for each length L up to a maximum length. From model experiments on the computer we conclude that five wavelengths are sufficient to produce such unique sets for lengths up to one meter. The wavelengths must be chosen judiciously for best performance. Errors in the fractional fringe data reduce the usable column lengths. We have set up a computer program which accepts five frequencies f_n and the corresponding values of $\sin g_n$ and $\cos g_n$, generates a table of $n\lambda_n + g_n\lambda_n/2\pi$ and compares it with the input data. A tolerance for the comparison can be set. The lowest n for which a matching set can be found is printed out. With the knowledge of n the length L can then easily be calculated. An example is given in Appendix B.

TEMPERATURE EFFECTS

The ultrasonic transit time t through the column (path length $2L$) is

$$t = \frac{2L}{c}$$

its dependence on temperature T is given by

$$\frac{dt}{t} = \frac{\alpha dT}{1 + \alpha T} - \frac{\beta dT}{1 + \beta T}$$

where α is the thermal expansivity and β is the temperature coefficient of the speed of sound. With $\alpha = 1.87 \times 10^{-4} \text{ K}^{-1}$ and $\beta = -3.18 \times 10^{-4} \text{ K}^{-1}$

$$\frac{dt}{t} = 5 \times 10^{-4} \times dT.$$

A temperature change of $dT = 1\text{K}$ causes a change in the transit time of 5×10^{-4} or 0.05%. Generally not the transit time but a harmonic of the resonance frequency near 10 MHz is measured. This measurement can be made to about 4×10^{-7} (4 Hz in 10 MHz). Since the above temperature coefficient applies also to the frequency, except for a sign change, a temperature stability of .8 mK is required to fully exploit the sensitive frequency measurement.

To illustrate the effect of the diurnal temperature cycle assume that the temperature drops by 1K over an 8 hour period. This then causes a frequency drift of about -10 Hz/min. Measurements are presently taken manually and therefore slowly. Each time measurements are taken one must also determine the frequency drift with time and correct the measured frequencies for the temperature drift effect.

In the future we expect to control the data acquisition with a MIDAS process controller. This should accelerate the collection of data and reduce the temperature drift effect. However, a very tight temperature control will always be necessary for accurate column length measurements. For an uncertainty in the length determination of 1 ppm the temperature must be stable and known to better than 2 mK.

THE SPEED OF SOUND IN MERCURY

Preliminary measurements of the speed of sound in mercury were made. The ultrasonic transit time was measured with the fringe counting interferometers. The column length was measured by detecting the position of the mercury meniscus with a telescope and reading the position from a vertical scale by rotating the telescope about its vertical axis. The scale had previously been calibrated with a laser to better than .01 mm. Great care was taken to reduce all errors connected

with the rotation of the telescope. It was found that the mercury meniscus could be located reproducibly by using a properly lit white backdrop with black marks behind the column. The temperature of the manometer was measured with two platinum thermometers, one on the reference plate and one on the upper part of the column.

The speed of sound was calculated from

$$c_o = \frac{(\ell_2 - \ell_1) 8 f}{(n_1 - n_2) + \alpha [n_o (\Delta T_1 - \Delta T_2) + n_1 \Delta T_1 - n_2 \Delta T_2]}$$

where n_o is the length of the mercury column below the lowest reading position measured in $\lambda/8$, L_1 and L_2 are the corrected scale readings, f frequency of carrier, n_1 and n_2 counter readings at ℓ_1 and ℓ_2 respectively, α is the temperature coefficient of velocity, $\Delta T = T - T_{ref}$, $T_{ref} = 23^\circ\text{C}$.

In the present set-up $l_0 = 48$ mm and therefore $n_o = 2648$ with $\lambda = .145$ mm. Two series of measurements were made. Sufficient data to illustrate them is given in Appendix C. The results are summarized in Table I. To obtain an estimate of the systematic uncertainty we form the total differential of the equation for the speed of sound c_o

$$\frac{dc_o}{c_o} = \frac{2d\ell}{\ell} + \frac{df}{f} + \frac{1}{n_1 - n_2} [2dn + n_1 \Delta T_1 d\beta + n_1 \beta d\Delta T + \Delta T_1 \beta dn].$$

Our estimate for the variances of the parameters is

$$d\ell = .03 \text{ mm}$$

$$d\beta = 3 \times 10^{-5} \text{ K}^{-1}$$

$$df = 2 \text{ Hz}$$

$$d\Delta T = .05 \text{ K}$$

$$dn = 1 \text{ count}$$

The variance $d\ell$ is included in the random uncertainty. The root sum square (RSS) of the ^{other} terms of dc_o is

$$\text{RSS} = \frac{7.5 \times 10^{-5}}{2.6 \times 10^{-5}}$$

and the resultant estimate of the uncertainty of c_o is

$$S(c_o) = \frac{0.04}{.11} \text{ m/s.}$$

We have then for the speed of sound in mercury contained in a glass tube with an internal diameter $D=350\lambda$ and at 23°C

$$c = 1449.57 \text{ m/s}$$

with a random uncertainty of 0.04 m/s and a systematic uncertainty of $\frac{0.04}{11} \text{ m/s}$.

Several measurements of the speed of sound in mercury have been reported in the literature, but all of them lack an indication of the uncertainty of measurement. They are listed nevertheless in Table II.

ELECTRONIC APPARATUS

Fig. 8 shows a block diagram of the electronic apparatus currently in use. Most of the components have been described in the preceding annual report. Only the limiter, the counter and the failure detector shall be discussed here.

The limiter is used to compress the variable amplitude signal (Fig. 6.a to 6.l) sufficiently to render the input signal to the phase sensitive detectors constant. This ensures that the output from the filter is standardized regardless of the column length. Consequently either one of the filter output signals can be used for interpolation and also a failure signal can easily be derived. Fig. 9 shows the output from the limiters for three column lengths. The amplitude of the first echo is independent of column length up to the maximum length of 1100 mm.

A failure indicator was designed to actuate an alarm or ~~annunciator~~ ^{annunciator} whenever the magnitude of the vector (u_1, u_2) falls below a certain level. The level was selected to allow trouble free operation of the counter. The failure indicator consists essentially of two squarers and an adder plus some additional logic circuitry. The failure indicator is very helpful in avoiding erroneous counts when the interferometer runs unattended.

With the help of the failure detector we could show that the up/down counter used until recently generated occasional, erroneous counts from noise and from jitter in the input signals. A new counter employing a novel anti-jitter circuit and quadrature detector was therefore designed and bread-boarded. The counter contains memory elements and can therefore operate without the sample and hold amplifier and filters. The read-out design has not been completed yet.

FUTURE WORK

We plan to complete the design of the new up/down counter including printed circuit board layout and will assemble several counters for use with the manometer.

We will complete the electronics for operation of all three columns and for control and data acquisition by means of a process controller.

We plan a more accurate measurement of the speed of sound using a laser interferometer instead of the scale.

We will make measurements of the speed of sound in glass tubes with different diameters.

We expect to begin operating the instrument as a standard manometer with an accuracy essentially limited by our current knowledge of the speed of sound in mercury.

Longer range plans include a consolidation of the electronic circuitry into one single-purpose package and the design and construction of an air thermostat of sufficient stability. Also we plan to extend the column length to a total of 2.5m.

LIST OF FIGURES

- Fig. 1 W-tube ultrasonic manometer.
- Fig. 2 Bottom closure.
- Fig. 3 Dependence of apparent attenuation on tilt;
(a) horizontal, (b) tilted $.04^\circ$.
- Fig. 4 Pneumatic connections.
- Fig. 5 First echo amplitude (a) and decrement (b) as function of column length.
- Fig. 6 Echo sequences for various column lengths; sweep rate adjusted to show three echos; amplification constant.
- | | |
|------------|-------------|
| (a) 100 mm | (g) 700 mm |
| (b) 200 mm | (h) 800 mm |
| (c) 300 mm | (i) 900 mm |
| (d) 400 mm | (k) 1000 mm |
| (e) 500 mm | (l) 1100 mm |
| (f) 600 mm | |
- Fig. 7 Interpolation
- Fig. 8 Block diagram of electronic apparatus
- Fig. 9 Limiter output for three column lengths;
(A) 1100 mm, (B) 550 mm, (C) 60 mm.
- Table I Results of speed of sound measurements
- Table II Speed of sound in mercury at 23°C
- Appendix A Determination of L with critical frequencies
- Appendix B Fractional fringes
- Appendix C Data taken for the determination of the speed of sound in mercury.

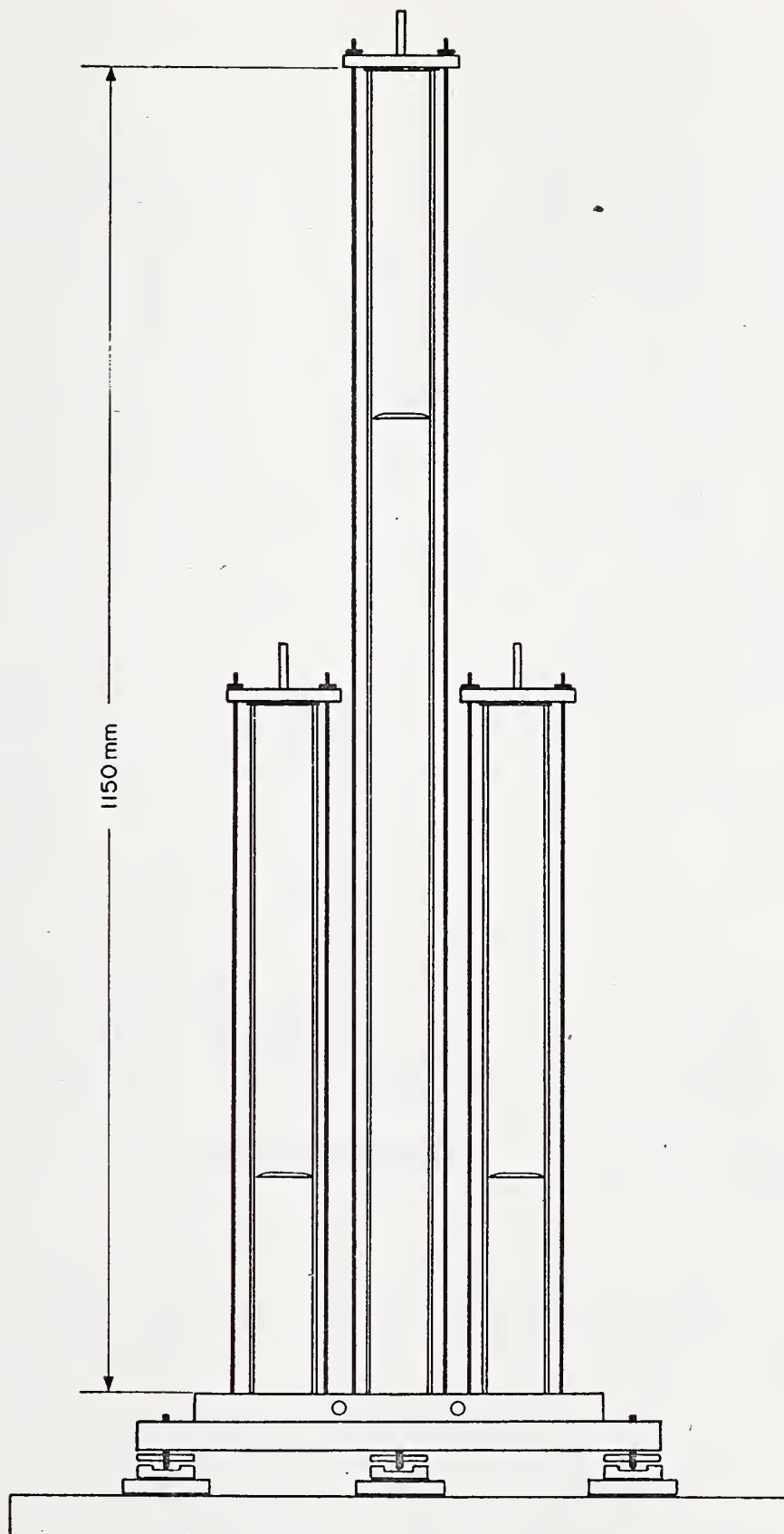


Fig. 1 W-tube ultrasonic manometer.

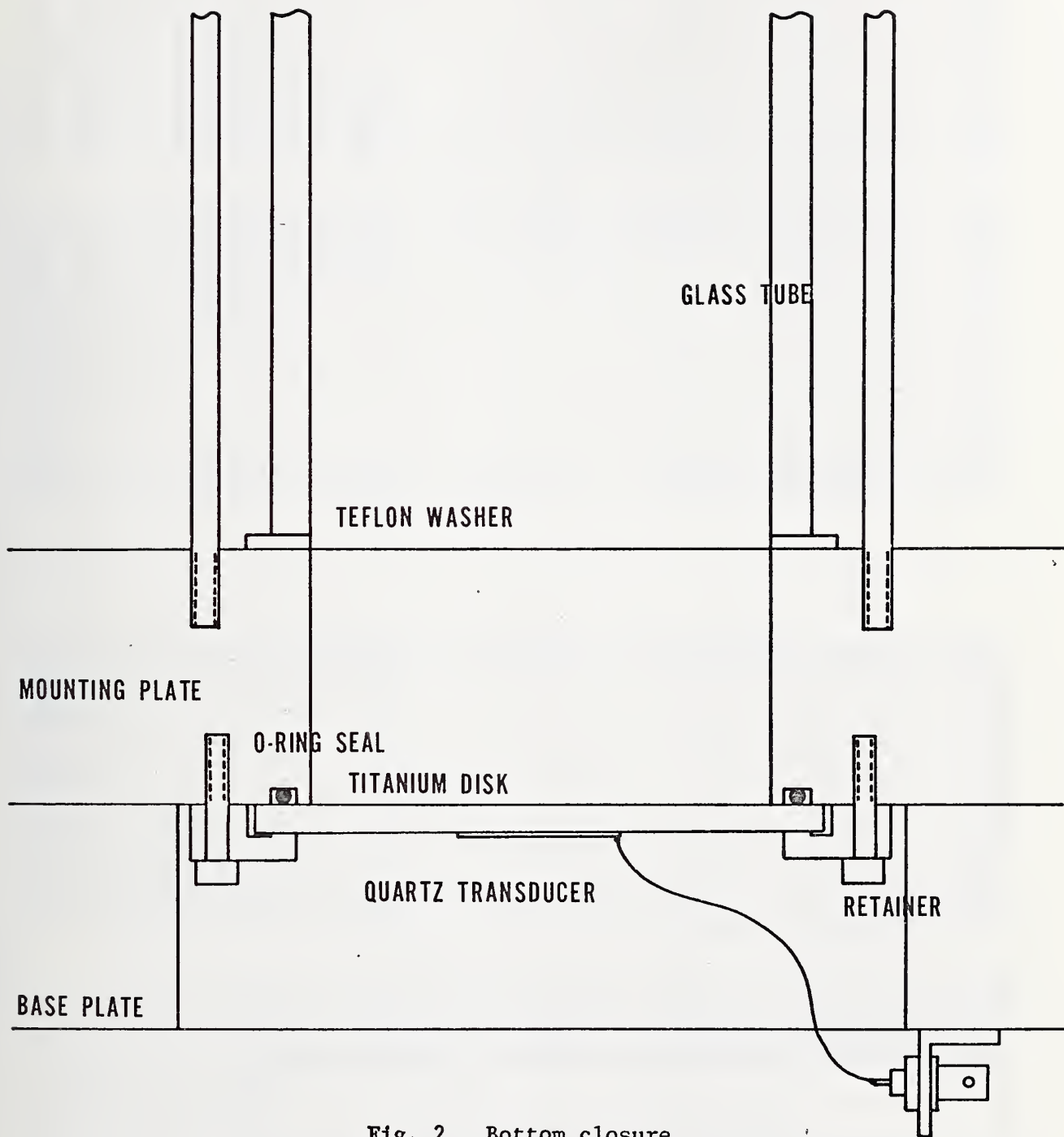


Fig. 2 Bottom closure.

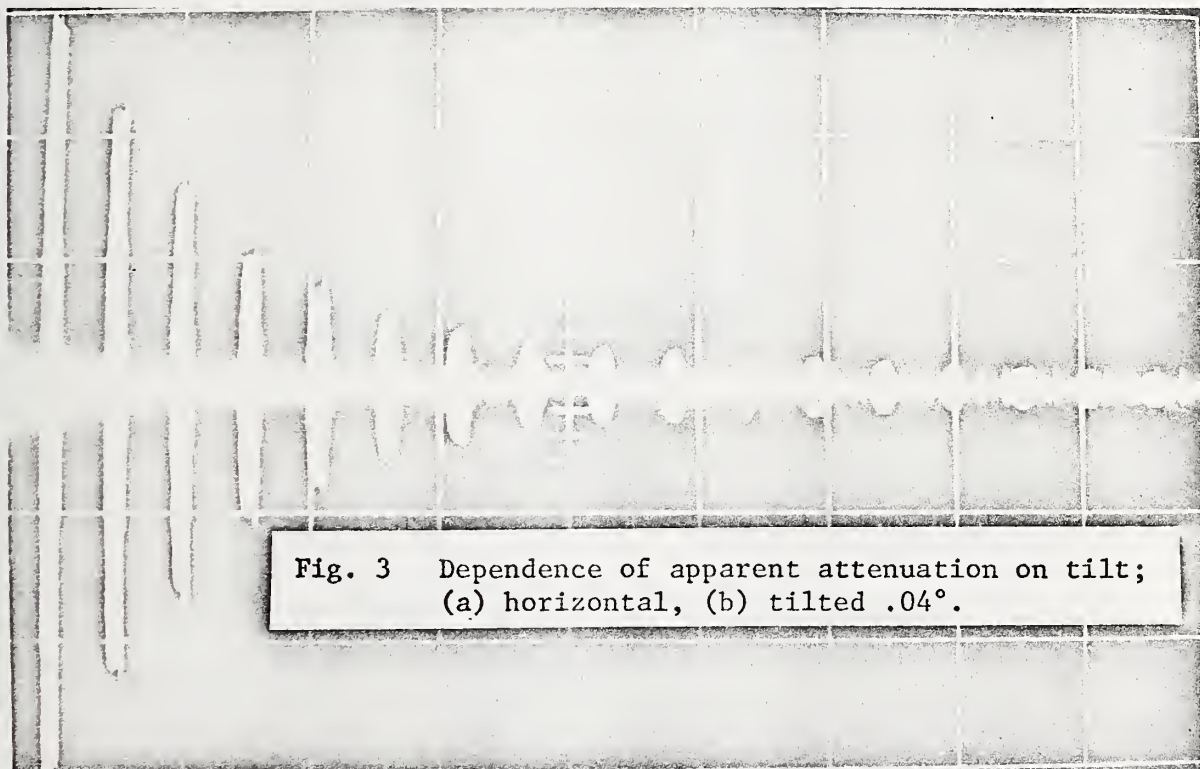


Fig. 3 Dependence of apparent attenuation on tilt;
(a) horizontal, (b) tilted $.04^\circ$.

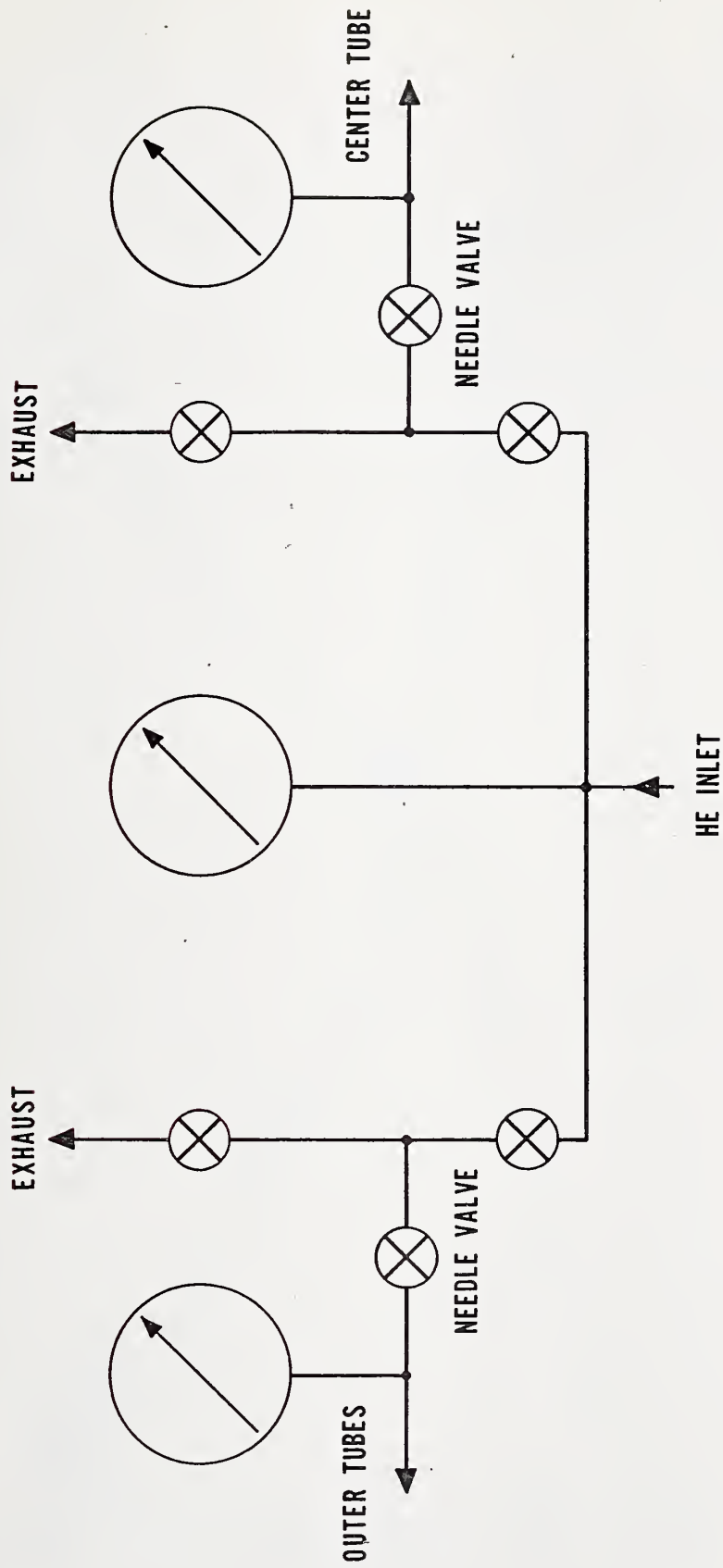


Fig. 4 Pneumatic connections.

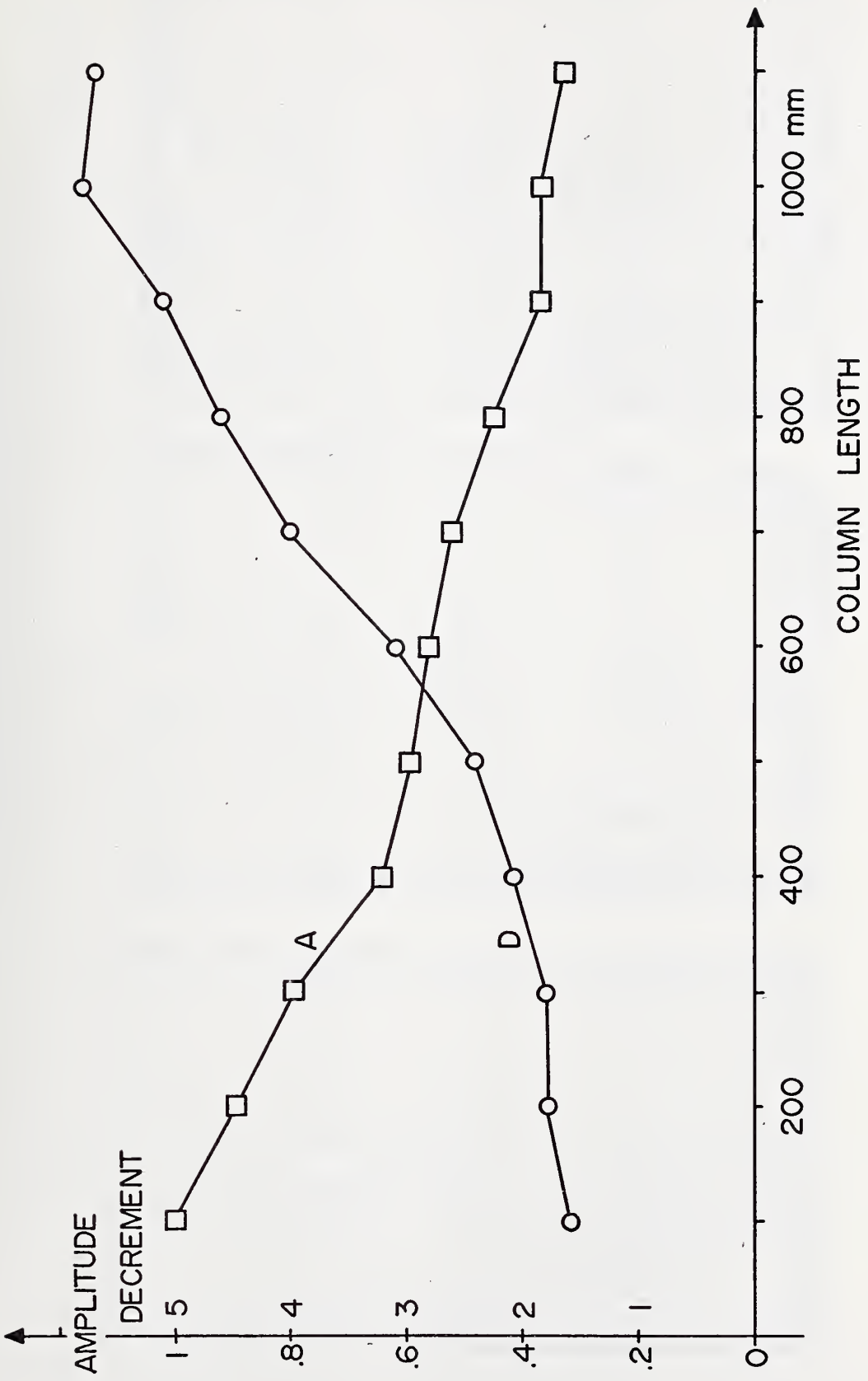


Fig. 5 First echo amplitude (a) and decrement (b) as function of column length.

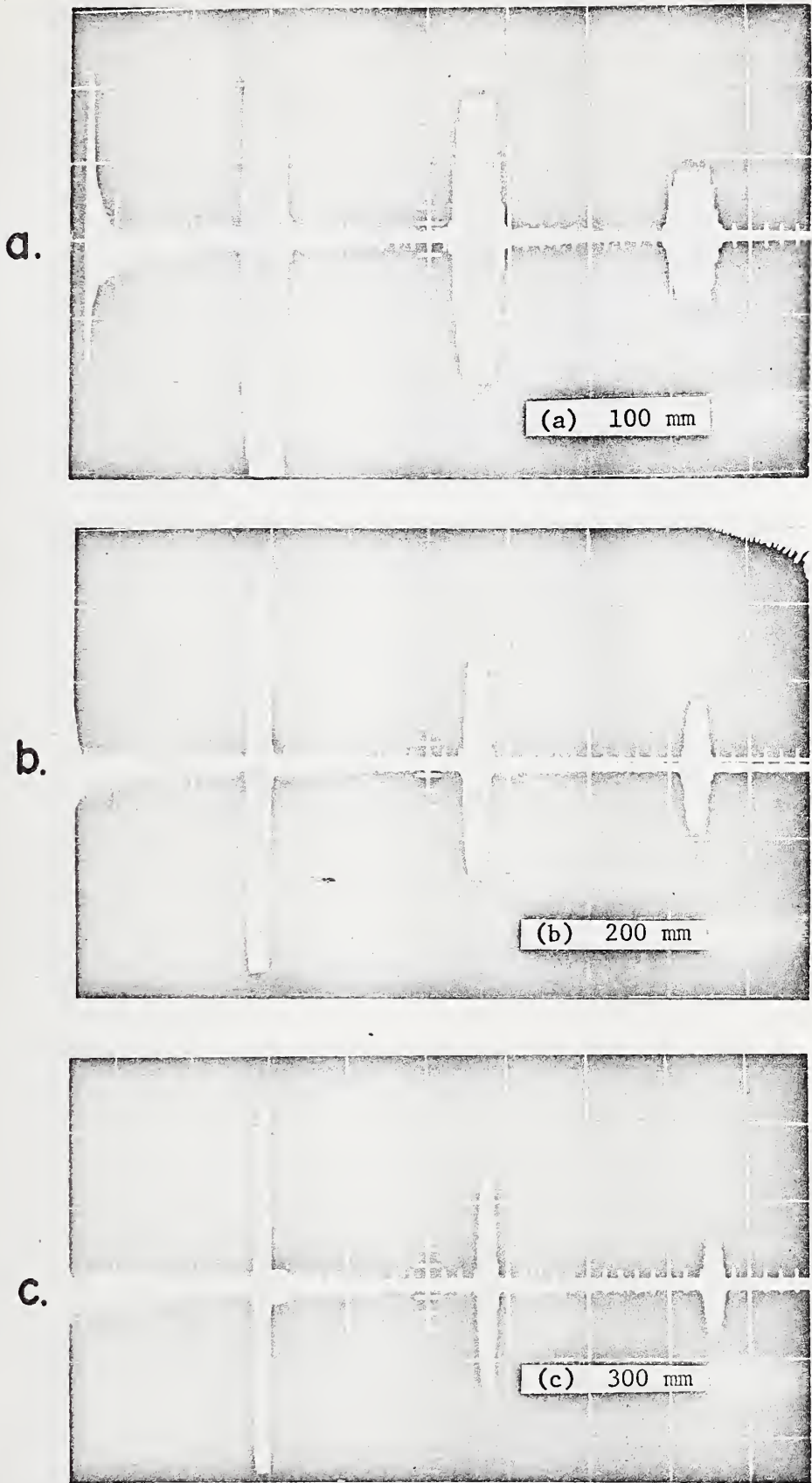
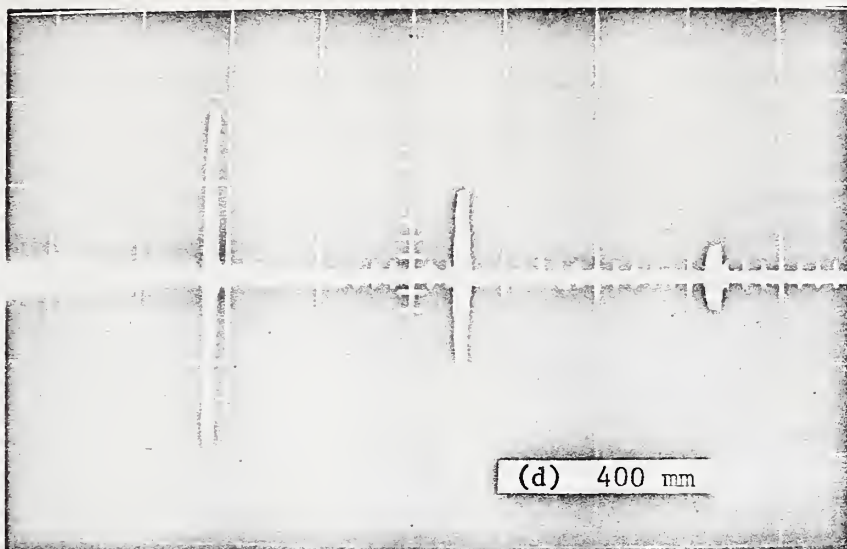
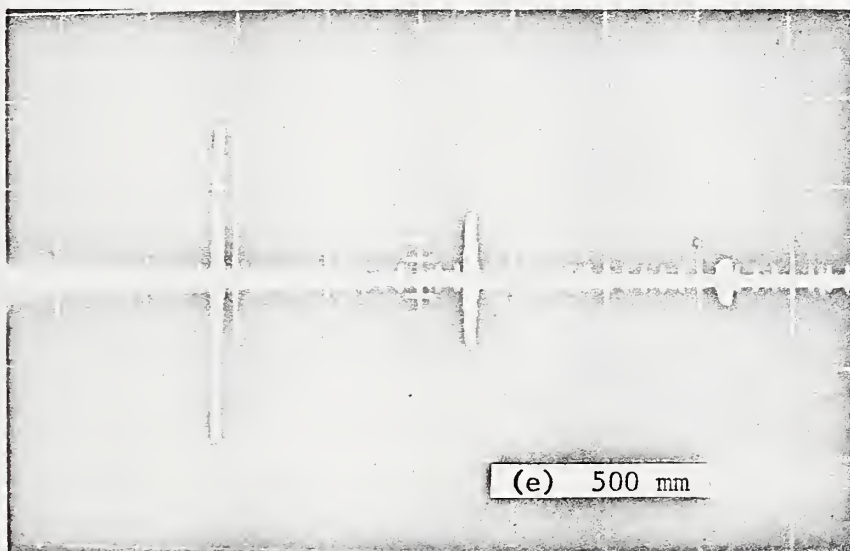


Fig. 6 Echo sequences for various column lengths; sweep rate adjusted to show three echos; amplification constant.

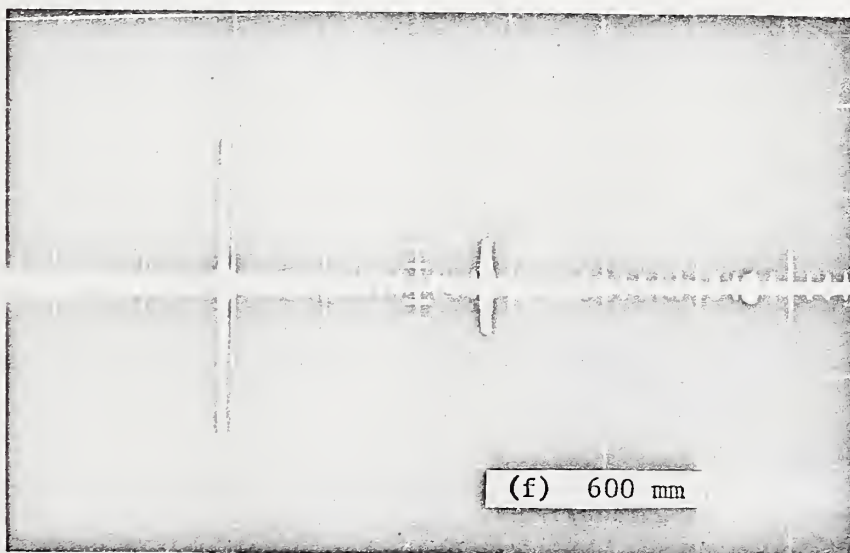
d.



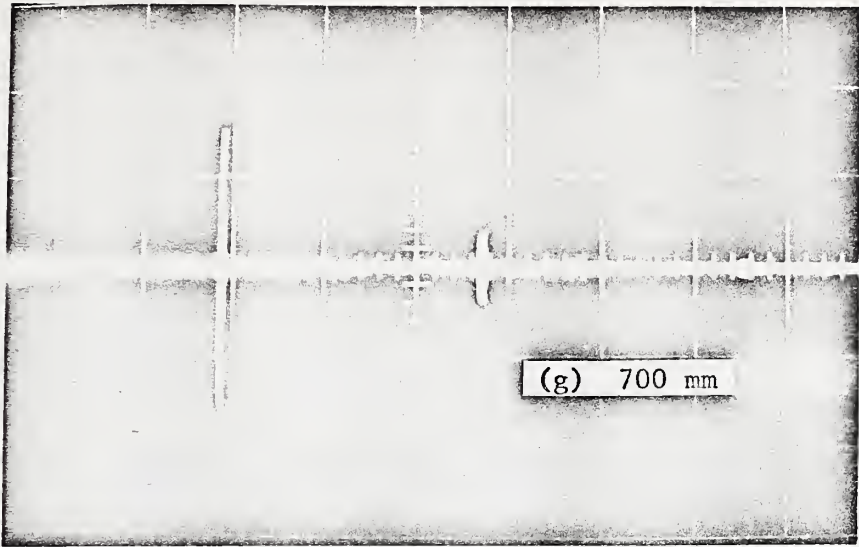
e.



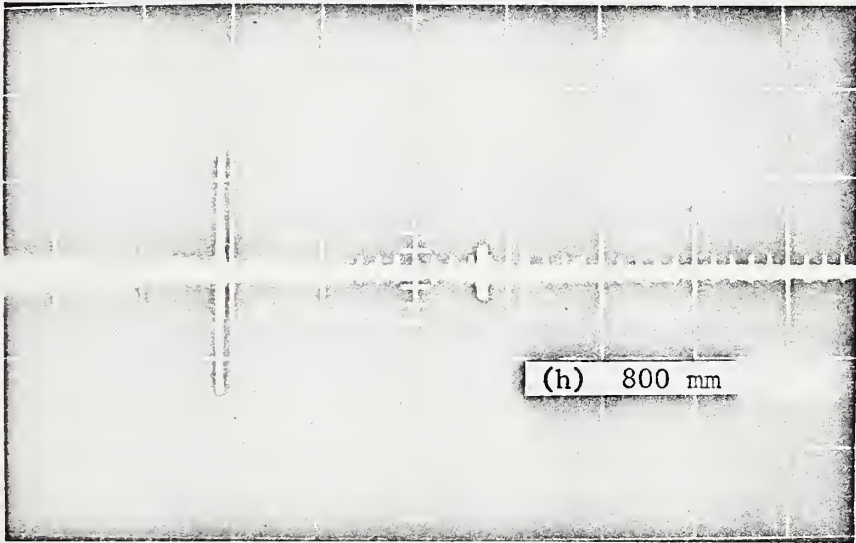
f.



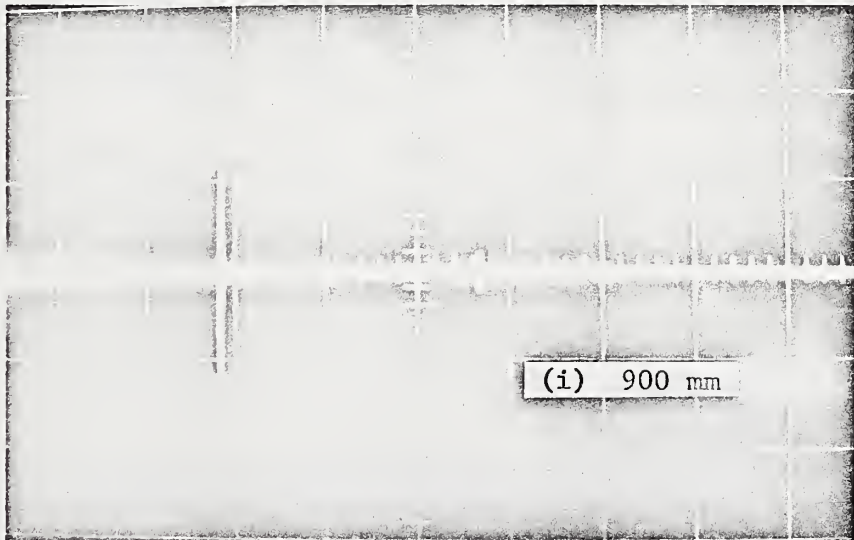
g.



h.



i.



k.



l.



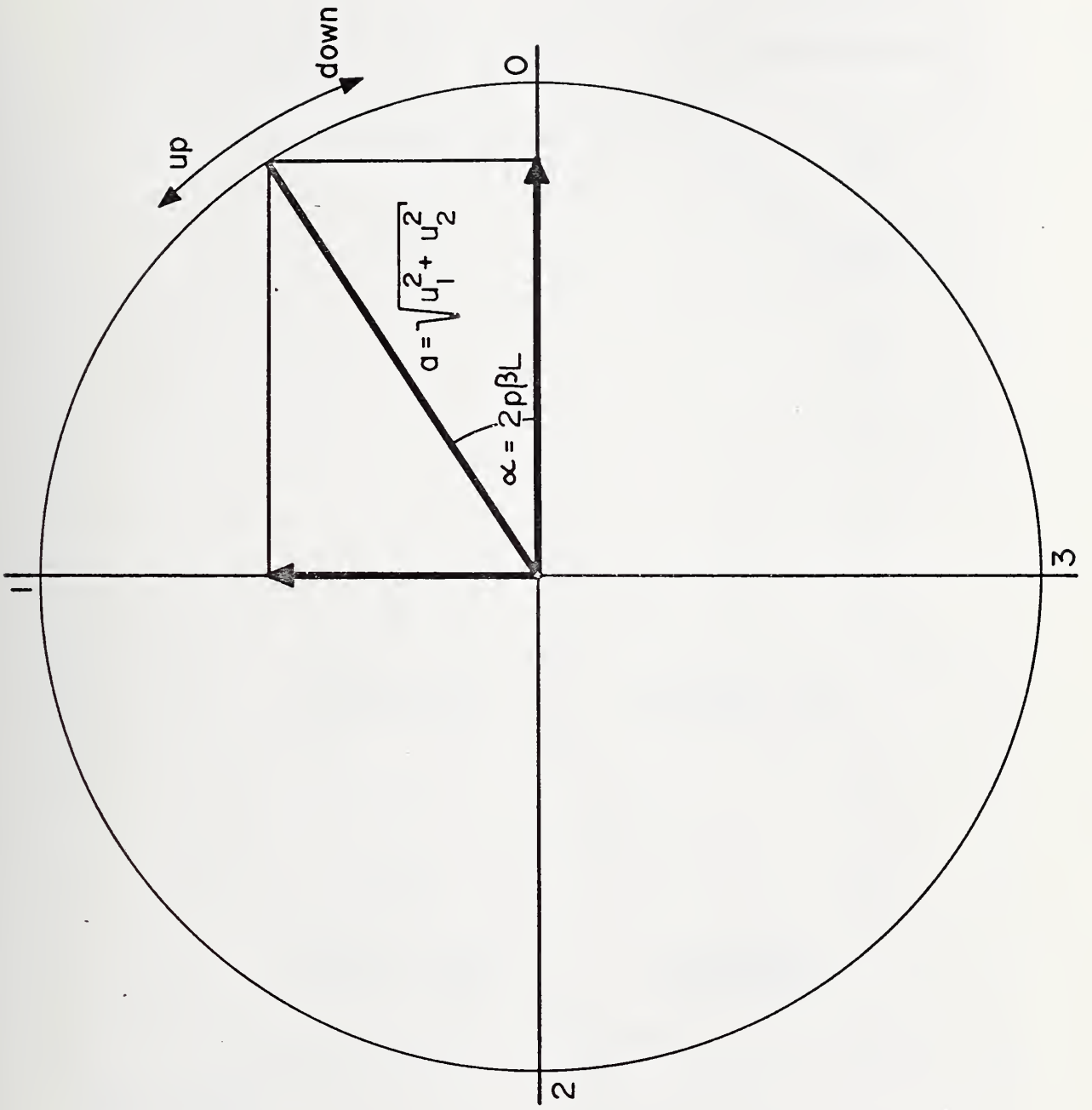


Fig. 7 Interpolation

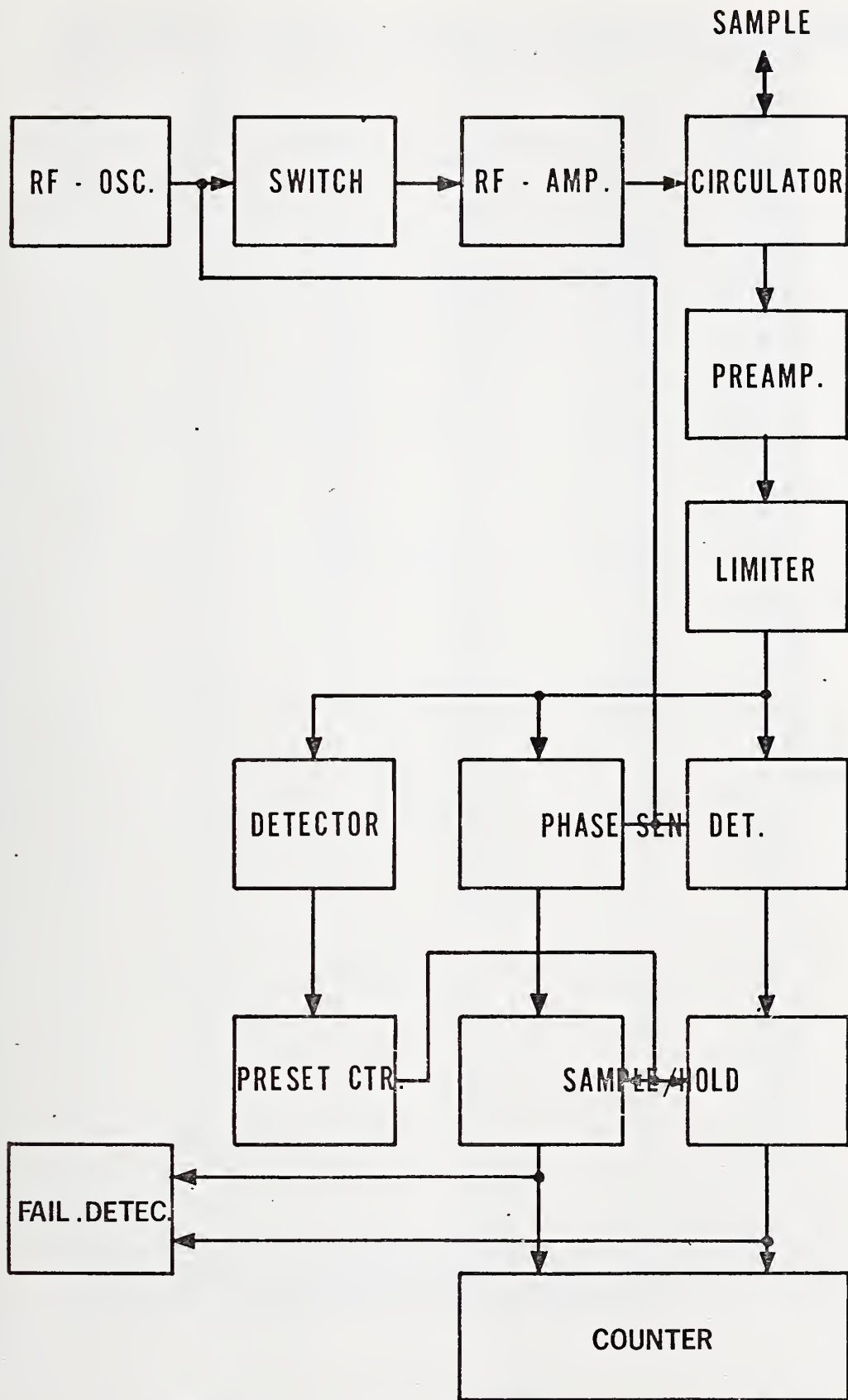
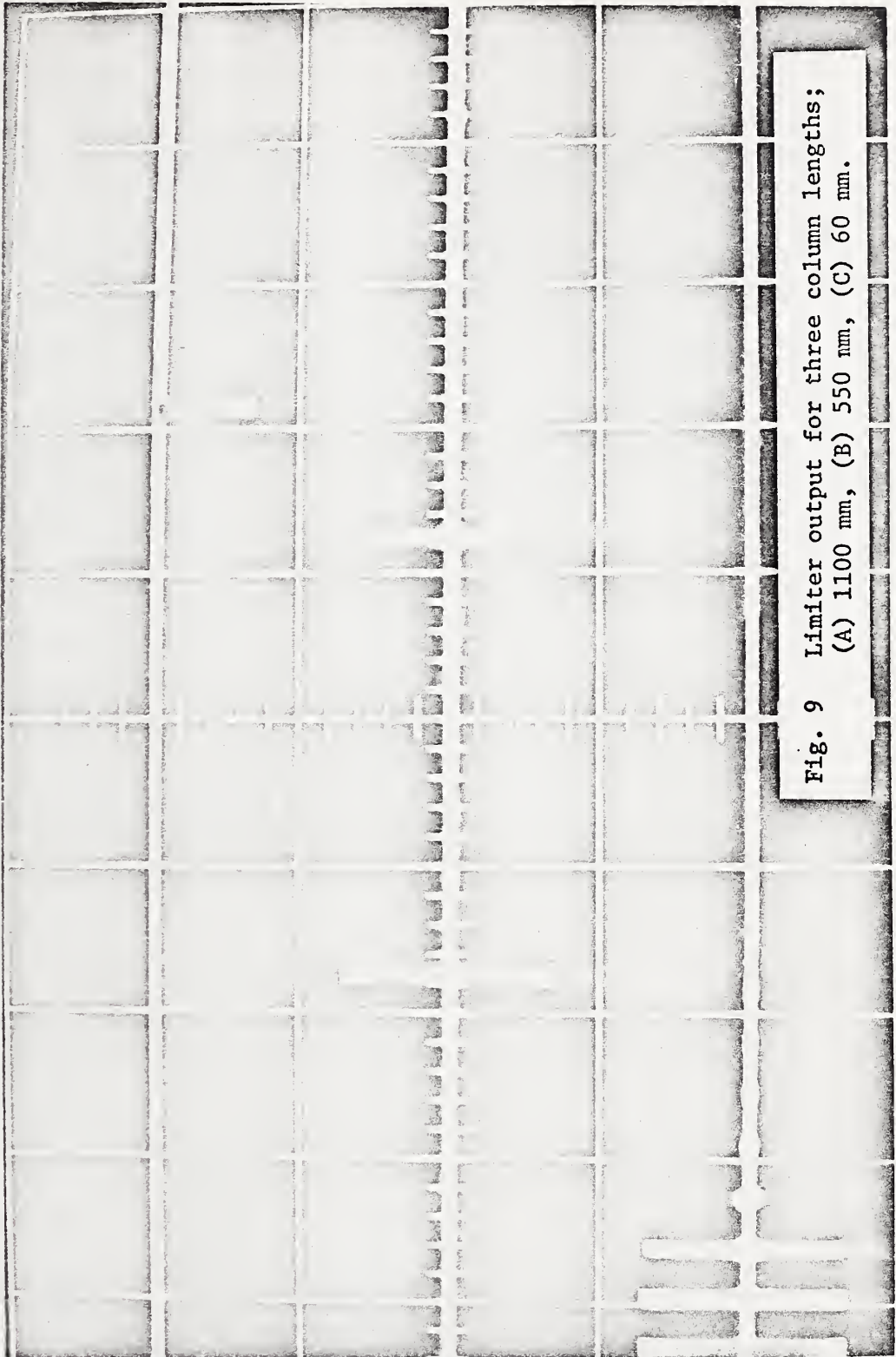


Fig. 8 Block digram of electronic apparatus



A

B

C

Fig. 9 Limiter output for three column lengths;
(A) 1100 mm, (B) 550 mm, (C) 60 mm.

TABLE I. Results of speed of sound
measurements in mercury

First set of data:

#	c	v	v ²
2/3	1449.66 m/s	+9	81
5/6	1449.68 m/s	+11	121
6/7	1449.51 m/s	-6	36
7/8	1449.49 m/s	-8	64
8/9	<u>1449.53 m/s</u>	-4	<u>16</u>
mean	1449.57 m/s	S =	318

standard deviation of the mean $d = .04$ m/s

Second set of data:

#	c	v	v ²
11/12	1449.73 m/s	16	256
13/14	1449.64 m/s	7	49
14/15	1449.50 m/s	-7	49
15/16	1449.52 m/s	-5	25
16/17	<u>1449.47 m/s</u>	-10	<u>100</u>
mean	1449.57 m/s	S =	<u>479</u>

standard deviation of the mean $d = .05$ m/s.

Standard deviation of the mean of ten measurements $d = .03$ m/s

TABLE II. Speed of Sound in Mercury at 23°C

Experimentor	c[m/s]
this report	1449.57
Coppens et al	1449.69
Freyer et al	1449.6
Hill et al	1450.7
Hunter et al	1452

A.B. Coppens, R.T. Beyer, J. Ballou
 JASA 41, 1443 (1967)

E.B. Freyer, J.C. Hubbard, D.W. Andrews
 J. Am. Chem. Soc. 51, 759 (1929)

J.E. Hill, A.L. Ruoff
 J. Chem. Phys. 43. 2150 (1965)

J.L. Hunter, T.J. Welch, C.J. Montrose
 JASA 35, 1568 (1963)

all values were reduced to 23°C using the temperature coefficient $\alpha = -3.20 \times 10^{-4} \text{ } ^\circ\text{C}^{-1}$ reported by J.C. Hubbard and A.L. Loomis in Phil. Mag. 5, 1177 (1928).

APPENDIX A

DETERMINATION OF L WITH CRITICAL FREQUENCIES

DATA:

#	time	fringe ct.	frequency	frequency corrected for dT
1	18.23	0	9900520	
2	18.24	0	9900509	9900509
3	18.25	0	9900502	9900508
4	18.26	0	9900498	9900510
5	18.27	41	9927196	9927214
6	18.28	92	9960398	9960422
7	18.29	-	-	-
8	18.30	-	9900475	9900511
9	18.31	0	9900469	9900511
10	18.32	33	9921958	9922006
11	18.33	97	9963619	9963673
12	18.34	-	9901759	9901819
13	18.35	0	9900445	9900511

COMPUTATION:

Points 2, 3, 4, 8, 9 and 13 taken at the same fringe

$$\frac{\Delta f}{\Delta t} \sim 6 \text{ Hz/min (temperature drift)}$$

$$\frac{f_{n+41} - f_n}{41} = f_{1,1} = 651.317 \text{ Hz}$$

$$\frac{f_{n+92} - f_n}{92} = f_{1,2} = 651.217 \text{ Hz}$$

APPENDIX A (Cont'd)

$$\frac{f_{n+33} - f_n}{33} = f_{1,3} = 651.364 \text{ Hz}$$

$$\frac{f_{n+97} - f_n}{97} = f_{1,4} = 651.155 \text{ Hz}$$

$$\text{average } f_1 = 651.263 \text{ Hz}$$

$$f_n / f_1 = 15202.01 \approx 15202$$

$$f_1 = \frac{f_n}{n} = 651.2636$$

$$L = \frac{c}{2f} = 1.11322 \text{ m}$$

APPENDIX B
FRACTIONAL FRINGES

DATA:

sin g	cos g	f
.999	.000	9956680.0
.999	.000	9954076.0
.999	.000	9951474.7
.999	.000	9950820.7
.999	.000	9949517.4

L = 1.110216 m

APPENDIX C

Data taken for the determination of the speed of sound in mercury

#	Time t	Scale temp., °C T ₁	Scale temp., °C T ₂	Hg temp., °C R ₃	Hg temp., °C R ₄	Hg temp., °C T ₃	Hg temp., °C T ₄	counter	scale, mm H	corr. scale H ₂₃ (mm)
2	09.22	22.98	22.99	109.0860	109.0200	23.006	22.862	-00590	21.98	21.99
3	10.25	22.97	22.90	109.0718	109.0181	22.960	22.857	45243	852.48	852.55
5	10.34	22.97	22.90	109.0718	109.0181	22.960	22.857	45798	852.00	852.07
6	11.25	22.98	22.92	109.0736	109.0218	22.960	22.866	-00434	25.15	25.16
7	12.25	22.92	22.95	109.0637	109.0127	22.810	22.843	44928	847.05	847.12
8	13.20	22.86	22.73	108.9880	108.9820	22.733	22.766	-00398	25.83	25.84
9	14.25	22.72	22.69	109.0085	108.9655	22.691	22.724	44968	847.83	847.90
<hr/>										
11	9.18	22.98	22.99	109.0818	109.0187	22.995	22.859	-00610	21.57	21.58
12	10.21	22.97	22.90	109.0674	109.0193	22.949	22.860	45253	852.65	852.72
13	10.32	-	-	109.0820	109.0185	22.986	22.858	45206	852.15	852.22
14	11.22	22.98	22.92	109.0719	109.0219	22.960	22.867	-00444	24.99	25.00
15	12.20	22.92	22.95	109.0582	109.0132	22.811	22.845	44940	847.28	847.35
16	13.17 b	22.86	22.73	108.9765	108.9824	22.734	22.767	- 411	25.58	25.59
17	14.18	22.72	22.69	109.0064	108.9656	22.691	22.724	44960	847.65	847.72

